Colloid Polym Sci 274:197–208 (1996)

ORIGINAL CONTRIBUTION

C. Tribout
B. Monasse
J.M. Haudin

Experimental study of shear-induced crystallization of an impact polypropylene copolymer

Received: 14 December 1994
Accepted: 5 September 1995

C. Tribout · B. Monasse
Prof. Dr. J.M. Haudin (✉)
Ecole Nationale Supérieure des Mines de Paris
Centre de Mise en Forme des Matériaux
Unité de Recherche Associée
au CNRS no 1374, B.P. 207
06904 Sophia-Antipolis Cedex, France

Abstract The crystallization kinetics of polypropylene was observed during shear and after shear experiments under isothermal condition. The crystallizations were performed in a plate-plate and a fiber pull-out device. The nucleation density, the crystalline growth and the overall kinetics were measured and compared with data obtained in a similar way but during static experiments. The morphologies are spherulitic and formed from nuclei which seem to be randomly distributed. α-phase spherulites are always observed but with a nucleation density and a growth rate which depend on shear-rate. The nucleation density is strongly enhanced by shear and acts as the main factor on the overall kinetics. The overall kinetics can be analyzed with a two-step Avrami model, where an Avrami exponent n_1 with a very high value is always observed first after shear and a more usual parameter n_2 for the subsequent crystallization period. This high value of n_1 seems to be related to the strong enhancement of nucleation density. The growth rate increases with the shear-rate, but the basic growth mechanisms do not seem to be modified. For crystallizations after shear the growth rate decreases with a long-time delay after shear but not down to the static value. The effect is characteristic of a partial relaxation of chain orientation after shear but with a very unusual time constant.

Key words Shear-induced crystallization – nucleation – growth – overall kinetics – polymer – polypropylene

Introduction

Study of flow-induced crystallization has drawn much interest because it implies the possibility of controlling and predicting the final morphologies and properties of semi-crystalline polymers in current transformation processes like injection-molding or extrusion. Due to flow, polymer chains are oriented in the melt and can crystallize with morphologies different from those encountered under quiescent conditions (observation of shish-kebab or row-nucleated structures rather than usual spherulites). In the 1970s a great effort was devoted to elucidate the fiber formation under elongational flow from dilute solutions of polymers [1]. Shear flow was often neglected as it was considered at that time as a "weak" flow, unable to provide extension of polymer chains and to induce fiber formation. However, in polymer melts even shear flow modifies the crystallization behavior and the resulting morphologies (acceleration of the overall kinetics of transformation [2–9], observation of shish-kebab structures [10]). For that reason some authors have been interested in understanding shear-induced crystallization. Experiments dealing with it are summarized in a non-exhaustive way in

Table 1 References on kinetics data from crystallization experiments performed on various polymers under shear, with the following abbreviations: high density polyethylene (HDPE); poly(1-butene) (PB−1); poly(ethylene oxide) (PEO); polypropylene (PP); poly(ε-caprolactone) (Pε–CL)

Polymer	$\bar{M}_w \times 1000$	Rheometer	Shear parameter	Crystallization temperature	Crystallization measurement	Reference
HDPE	70	Parallel-plate	stress	120–135 °C	Induction time	Haas, Maxwell [2]
PB–1	120		$1.4\,10^4$–$4.3\,10^5$ Pa	93–113 °C		
	260					
	500					
HDPE	50	Coaxial cylinders	rate	130–140 °C	Crystallization temperature under shear and cooling	Kobayashi, Nagasawa [3]
	2.7		2.7–1380 s^{-1}	102–112 °C		
PB–1	500	Parallel-plate	strain	85, 92 °C		Wereta, Gogos [4]
PEO	2.2	Coaxial cylinders	rate	52–60 °C	Induction time, Avrami coefficients	Fritzsche, Price [6]
	11.8		0–168 s^{-1}			
	395					
HDPE	140	Biconical	rate	134–142 °C	Induction time, nucleation, growth rate	Tan, Gogos [7]
			1.5–7.5 s^{-1}			
HDPE	189	Parallel-plate	rate		Induction time	Lagasse, Maxwell [8]
	920		0.02–20 s^{-1}	125–141 °C	Induction shear-strain	
	1860					
PP and random copolymer	350		0.5–4.2 s^{-1}	113, 121 °C		
PEO	2.2	Coaxial cylinders and rotational plate-plate	rate	50–56 °C	Conversion α	Fritzsche et al. [9]
	11.8		0–140 s^{-1}		Number of nuclei	
	395		0–22 s^{-1}			
HDPE	173	Coaxial cylinders	rate	130 °C		Andersen, Carr [11]
			0.07–0.4 s^{-1}			
PB–1	130	Rotational plate-plate	rate	95–105 °C	Nucleation rate Growth rate	Wolkowicz [12]
			0.2–12 s^{-1}			
PEO	12.6	Coaxial cylinders	rate		Avrami coefficients	Sherwood et al. [13]
	72.2		0–60 s^{-1}	56–60 °C	Number of nuclei	
Pε–CL	9.4		0–48 s^{-1}	48–51 °C		
HDPE	non defined	Coaxial cylinders	rate	129–135 °C	Induction strain	Krueger, Yeh [5]
			0.4–10 s^{-1}			

Table 1. Most of them use custom-made rotational rheometers and are concerned with the measurement of the induction time of crystallization [2, 5–8] because the onset of crystallization is relatively easy to characterize by an increase of the force or the transmitted torque. Some studies [6, 9, 13] have determined the fraction of transformed material versus time but few **in situ** measurements concern the density of nuclei formed under shear and the growth rate of the subsequent morphologies [12].

The aim of this work is first to collect data on the shear-induced crystallization of polypropylene concerning as well nucleation and growth rates measurements as the overall crystallization kinetics. Then, an attempt is made to find relationships between these two kinds of data.

Experimental

Material

The material used for this study was an ethylene-propylene block copolymer supplied by APPRYL Company in the form of pellets under the reference PP7228. The ethylene content is 12% by weight. The average molecular weights are: $\bar{M}_n = 54\,000$ g/mol and $\bar{M}_w = 290\,000$ g/mol. Such a copolymer, which is a grade for injection molding, is often referred to as an "impact polypropylene copolymer". It was chosen here because the present work was included in a project concerning injection molding, especially for

automotive applications [14]. This type of polymer is classically produced in a two-reactor system. Polypropylene homopolymer is made in the first reactor, while an ethylene-propylene rubber (EPR) is polymerized in the second one. In fact, the final molecular structure is much more complex, and its detailed analysis is a formidable task. Recent work [15] showed that an impact polypropylene copolymer was composed of isotactic polypropylene homopolymer, which was the main constituent, and of an EPR phase, but also of partially crystalline ethylene-propylene copolymers. A major component of the partially crystalline ethylene-propylene copolymers was an ethylene-rich copolymer containing between 0 and 8 wt% of propylene comonomer. Therefore, the term "block copolymer," which is widely used in practice is incorrect, and concerning crystallization phenomena such a product essentially behaves as a homopolymer polypropylene. This was actually shown, in quiescent conditions, in a previous work in which we have demonstrated for instance that the equilibrium melting temperature and the spherulite growth rate were the same for a homopolymer and so-called block copolymers [16].

Differential scanning calorimetry (DSC)

Some preliminary experiments were performed by differential scanning calorimetry (Perkin Elmer DSC 2 calorimeter) in order to characterize the crystallization and melting behavior of the copolymer under investigation. After heating at 10 °C/min up to 228 °C (i.e., $T_m^0 + 20$ °C, T_m^0 being the equilibrium melting temperature [17]), the samples were maintained at that temperature, in the liquid state, for 5 min, and then cooled down at a constant cooling rate ranging from 0.31 to 80 °C/min. After crystallization, melting curves were recorded for a heating rate of 10 °C/min.

Shear apparatus

The apparatus mainly used is a parallel-plate device put under a polarizing microscope Reichert Zetopan Pol with transmitted light. This device was especially designed and built for this kind of study [18, 19], and essentially consists of a Mettler FP 52 hot-stage for the heating system. Heating or cooling are regulated through the use of the Mettler FP 5 controller. With this equipment the cooling rate is limited to about 10 °C/min. Another thermocouple is used independently to measure the temperature and to verify that it remains constant during isothermal crystallization under shear flow. The temperature is calibrated under static conditions by using a standard for thermometry (benzoic acid, melting temperature $T_m = 122.2$ °C). The temperature can be controlled to $\pm$ 0.1 °C. The polymer sample is sheared between two parallel glass slides at a constant shear-rate $\dot{\gamma}$, the simple-shear flow being induced by the movement of the lower one at a constant speed. The displacement of the slide is provided by a motor. Two different motors are used and allow shear-rate ranges which are respectively 0–2 s^{-1} and 2–26 s^{-1}, for a sample thickness of 200 μm. By construction the shearing time is limited to 60 s for the maximum speed of the first motor and 3 s for the second one.

The main aspects of such a device compared with classical rotational rheometers have been discussed in ref. [8]. Advantages of the parallel-plate shearing device can be summarized as follows:

- the use of thin samples minimizes the viscous heating and allows higher cooling rate down to the crystallization temperature;
- the control of temperature is better.

On the other hand, a major disadvantage is that the shearing time and subsequently the shear-strain are limited to fixed and finite values.

Experimental procedure for shear experiments

The specimens for the shear-induced crystallization experiments with the apparatus described above are prepared from a 300 μm-thick solid film with the following dimensions: length 30 mm, width 4 mm. The film is melted in the shear machine in static condition up to 210 °C, i.e., above the equilibrium melting temperature ($T_m^0 = 208$ °C [17]), and pressed to the final thickness ($e = 200$ μm) imposed by the machine. The shear direction of the apparatus is oriented at 45° from the polarizers directions to favor light depolarization during the crystallization under shear. After 5 min the polymer is cooled in static condition down to the crystallization temperature T_c. The shear experiment begins as soon as the isothermal condition is reached, i.e., at a time t_0 (Fig. 1). The measurement of the light intensity coming from the polymer birefringence then begins up to the end of crystallization. The shear is applied from t_0 to t_s (Fig. 1). Photographs are taken from time t_s simultaneously with light measurement to the end of crystallization. Morphologies, nucleation parameters (density of nuclei, nucleation rate) and growth-rate measurements are deduced from photographs and the overall kinetics from light measurements. Therefore, the overall kinetics is determined during the whole crystallization experiment (under and after shearing for $0 \leq \dot{\gamma} \leq 26\ s^{-1}$), while nucleation and growth parameters are measured only after shearing (for $0 \leq \dot{\gamma} \leq 2\ s^{-1}$). It is important to notice that

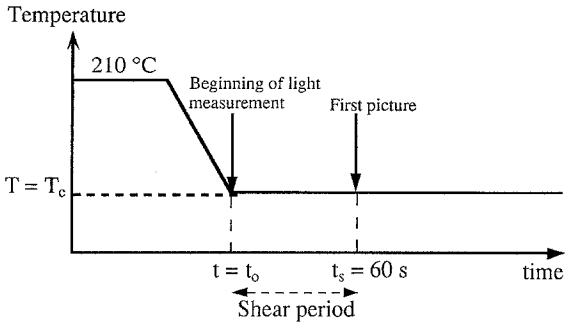

Fig. 1 Experimental scheme for crystallization after previous shear

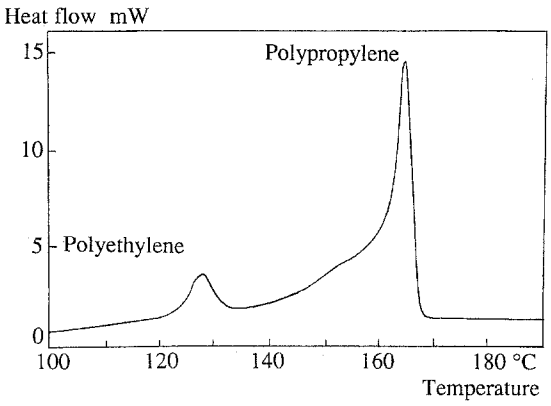

Fig. 2 Melting curve of PP7228 after crystallization at a 0.31 °C/min cooling rate

the growth rate is measured only after the cessation of flow. This procedure is justified by the profusion of small morphologies produced by shear. Consequently the growth-rate measurement of any spherulite during the shear flow is difficult. Such troubles have been already reported [12] and could explain the lack of data concerning the growth rate under flow condition.

Four crystallization temperatures have been selected for this study: 130.4°, 133.9°, 136.4° and 138.5 °C. Temperatures higher than 138.5 °C have not been considered because quiescent crystallization requires a too long time. Below 130.4 °C crystallization under shear flow is too rapid and leads to the breaking up of the sample. Unless otherwise specified, the shearing time t_s is kept constant and equal to 60 s for the first motor ($0 \leq \dot{\gamma} \leq 2\ s^{-1}$) and to 3 s for the second one ($2 \leq \dot{\gamma} \leq 26\ s^{-1}$).

Crystallization under shear induced by a fiber

Complementary shear experiments are performed with a different device in a Mettler FP 52 hot stage. The shear is applied by pulling out a glass fiber (diameter about 17 μm) from a molten polymer maintained between two static parallel glasses [20]. As an effect of the geometry and the kinematics of the experiment, shear-rate is maximum at the surface of the glass fiber and rapidly decreases along the radius. The value of the local shear-rate along the radius is defined by the polymer rheology. If the viscosity is described by a power law, $\dot{\gamma}$ is given by the following equation:

$$\dot{\gamma} = \frac{1-m}{m} \frac{1}{r^{1/m}} \left[\frac{1}{r_f^{1-1/m} - r_e^{1-1/m}} \right] V_f \,, \qquad (1)$$

where V_f is the velocity of the glass fiber; r_e and r_f are the external and the fiber radii, r is the location in the polymer ($r_f \leq r \leq r_e$; for $r = r_e$, the axial component of the velocity field vanishes); m is the exponent in the viscosity power law equation.

The general procedure for shear-induced crystallization is the same for the glass fiber and the plate-plate device: the polymer is melted up to 210 °C, cooled down to the crystallization temperature T_c, and then sheared at T_c between times t_0 and $t_s = t_0 + 30$ s. Nevertheless, with the glass fiber, morphologies can be observed and their radial growth rates measured both under shear and after cessation of shear. The velocities of the glass fiber are $V_f = 0.078$ mm/s and 0.3 mm/s, which leads to $\dot{\gamma} = 10\ s^{-1}$ and $\dot{\gamma} = 78\ s^{-1}$ at the fiber surface, respectively.

Results

Melting behavior

Figure 2 shows a typical melting curve of PP7228, recorded after crystallization at 0.31 °C/min. Two peaks can be distinguished. The smaller, at about 128 °C, corresponds to polyethylene, or at least to an ethylene-rich component. The larger, at about 164 °C, is typical of the α phase of a polypropylene homopolymer, which is in agreement with our above statements on the chemical composition of the product. In the following sections, only the crystallization of polypropylene will be considered and analyzed using thermodynamical and kinetic data for polypropylene homopolymer [17, 21].

Nucleation and growth

As under static condition, the entities observed in our shear experiments are always spherulites crystallized in the monoclinic α phase of polypropylene. Unlike the case

of polyethylene studied in refs. [18] and [19], these spherulites exhibit circular shapes. They are generally distributed at random, but in some cases they tend to be aligned along the flow direction.

The effect of shear on nucleation is characterized in the following two ways:

- measurement of the density of activated nuclei as a function of time, and especially of the final density of nuclei;
- determination of the nucleation rate.

The nuclei formation under shear condition as a function of time is determined according to the following procedure. For given crystallization conditions (temperature, shear-rate), micrographs are taken at different times t_{ph}. As shear may induce the appearance of numerous and consequently small morphologies, the treatment of these micrographs requires the use of the image analysis technique. In the first step, enlarged prints of the original photographs are prepared in order that the smallest visible spherulites appear as circles with a diameter of about 1 mm, which means magnifications ranging from several hundreds to about one thousand. Because of the weak contrast of these prints, the spherulitic pattern is then re-drawn on tracing paper, the spherulites being reproduced as dark patches. Using such pictures which usually contain several hundreds of entities, the image analysis technique allows us to count the number of spherulites on the picture and to determine the area occupied by each of them, from which their radius R is deduced. It is then possible to establish histograms of the number of spherulites as a function of their radius R. These numbers are converted into densities by dividing them by the actual area observed on the picture and by the specimen thickness (Fig. 3). The radius R and the growth rate G, whose measurement will be described below, make it possible to calculate the activation time t_a of each spherulite by the relationship:

$$t_a = t_{ph} - \frac{R}{G}, \tag{2}$$

where t_a and t_{ph} are measured from the time t_0 of the beginning of shear under isothermal conditions. It becomes then possible to plot the number of activated nuclei as a function of time, as shown in Fig. 4 at $T_c = 138.5\,°C$ for various shear-rates. These $N_a = f(t)$ curves have a sigmoidal shape and tend towards an asymptotic value N_{af}, the final density of activated nuclei. In spite of this actual sigmoidal shape, the most important part of the curve can be approximated by a straight line. This quasi-linear variation implies that impingement of growing morphologies can be neglected in this range of conversion, which is in complete agreement with the morphological observations. The nucleation rate is defined as the slope of the linear part of the curves $N_a = f(t)$.

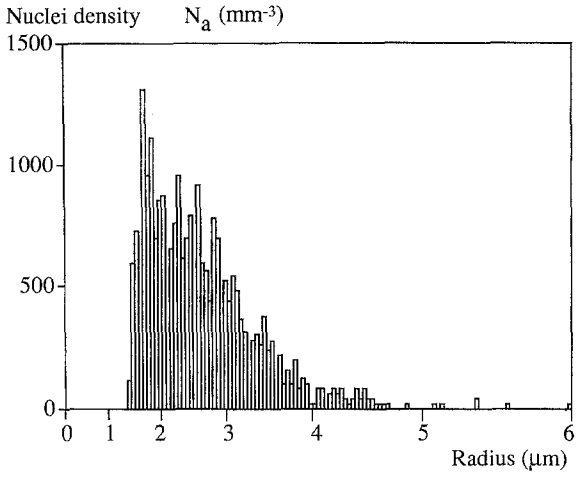

Fig. 3 Histogram of the number of spherulites per unit volume as a function of their radius ($T_c = 138.5\,°C$, $\dot{\gamma} = 2\,s^{-1}$). The radius scale is not linear because the histogram was primarily plotted as a function of the spherulite area

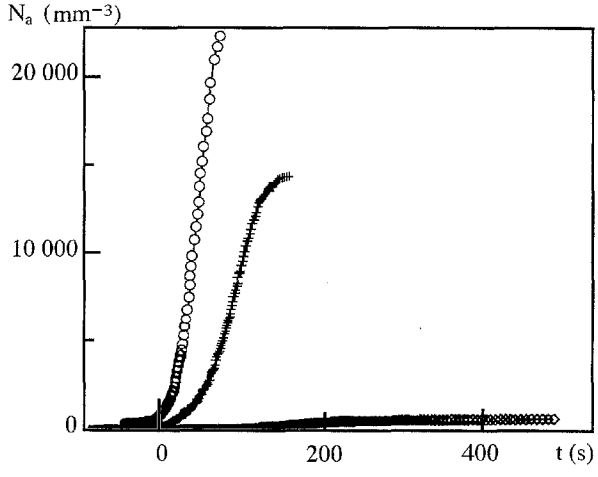

Fig. 4 Number of activated nuclei per unit volume as a function of time, $T_c = 138.5\,°C$: ◇ $\dot{\gamma} = 0.5\,s^{-1}$; + $\dot{\gamma} = 1\,s^{-1}$; ○ $\dot{\gamma} = 2\,s^{-1}$

In Fig. 5 N_{af} is plotted as a function of the shear-rate $\dot{\gamma}$ for three crystallization temperatures. For each crystallization temperature, the density of activated nuclei increases with increasing shear-rate up to a limit value, observed above $\dot{\gamma} = 1\,s^{-1}$. Even at low shear-rate ($\dot{\gamma} = 0.5\,s^{-1}$), the number of nuclei is higher than for quiescent condition. At $\dot{\gamma} = 2\,s^{-1}$, N_{af} is multiplied by about 100 with respect to the static case. Figure 6 shows the

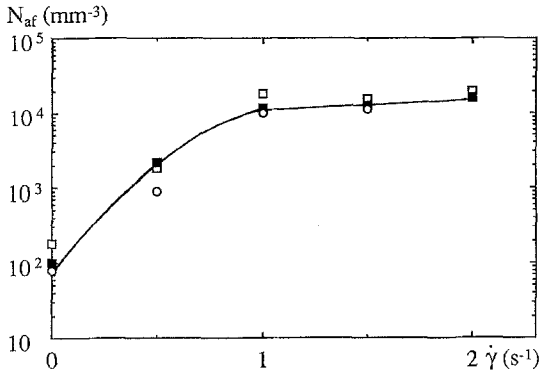

Fig. 5 Final number of activated nuclei per unit volume as a function of shear-rate, for three crystallization temperatures: □ $T_c = 133.9\,°C$; ■ $T_c = 136.4\,°C$; ○ $T_c = 138.5\,°C$

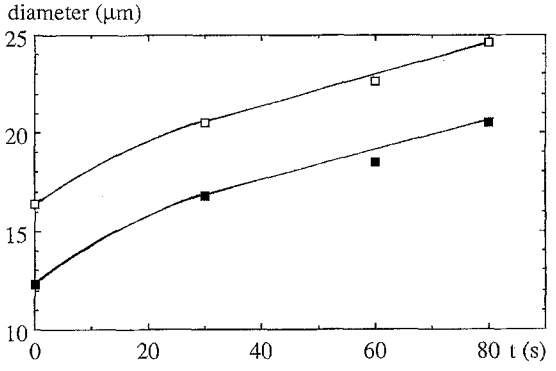

Fig. 7 Variation of the diameters of two spherulites as a function of time: $\dot{\gamma} = 1\,s^{-1}$; $T_c = 138.5\,°C$. The time origin corresponds to the cessation of shear

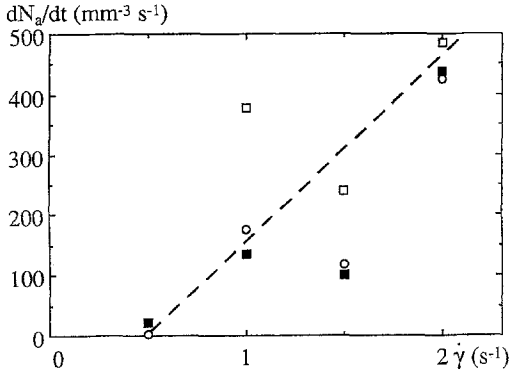

Fig. 6 Nucleation rate versus shear-rate for different crystallization temperatures: □ $T_c = 133.9\,°C$; ■ $T_c = 136.4\,°C$; ○ $T_c = 138.5\,°C$

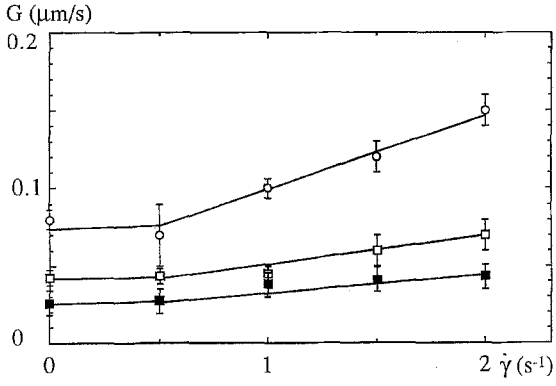

Fig. 8 Spherulite growth rate as a function of previous shear-rate: ○ $T_c = 133.9\,°C$, □ $T_c = 136.4\,°C$; ■ $T_c = 138.5\,°C$

nucleation rate determined as indicated above for various shear-rates at $T_c = 133.9°$, 136.4° and 138.5 °C. One notes an important scatter of the results, which originates from several causes: "natural" fluctuations of the number of activated nuclei from one experiment to another (for given crystallization conditions) and, of course, addition of experimental errors occurring at each step of the determination; for instance, the determination of the $N_a = f(t)$ curves requires the knowledge of the growth rate G, whose measurement is itself subject to uncertainty (see hereafter). Nevertheless, in view of these results, it can be stated that in this temperature range the nucleation rate strongly increases with shear-rate and is not significantly dependent on temperature. This general trend is represented by a dashed line in Fig. 6. In the same way, the density of activated nuclei at the end of crystallization is enhanced by the shear-rate, and not by the crystallization temperature (Fig. 5). Therefore, the shear-rate is the dominent parameter acting on the nucleation rate and on the density of activated nuclei.

For each crystallization temperature the growth rate is deduced from the variation of the spherulite diameters as a function of time. Figure 7 shows results after a shear-rate $\dot{\gamma} = 1\,s^{-1}$ at 138.5 °C. The growth rate decreases during the first 30 s after shear cessation to reach a constant value. This decrease will be discussed as an effect of a partial relaxation of the chain orientation. Whatever the crystallization temperature, the growth rates after shear are always larger than the values measured under static condition. These final constant growth rates are chosen for the future analysis. They correspond to long-term relaxation. These growth rates are analyzed at different temperatures as a function of previous shear-rate (Fig. 8). In addition to the experimental error due to the small spherulite size, it must also be noticed that a variable growth rate during a part of the experiment may have some influence on the determination of the nucleation parameters (see Eq. (2)). Nevertheless, this effect is expected to be of secondary importance with respect to the fluctuations of the number of activated nuclei.

Table 2 Crystalline growth rate measured under and after shear, and in static condition at two temperatures

Crystallization temperature	$\dot{\gamma}$ s^{-1}	Growth rate in μm/s quiescent condition	after shear condition	under shear condition
137.0 °C	10 s^{-1}	0.040 ± 0.005	0.060 ± 0.005	0.150 ± 0.050
140.0 °C	10 s^{-1}	0.018 ± 0.002	0.028 ± 0.005	0.100 ± 0.030

In order to avoid relaxation, growth-rate measurements are also performed under shear, by pulling the glass fiber inside the polymer melt (see the section "Experimental"). The same shear-rate $\dot{\gamma} = 10$ s^{-1} is applied during 30 s at two temperatures, $T_c = 137°$ and 140 °C, in order to compare the growth rates with data obtained under static and after shear conditions (Table 2). It can be shown that growth rate is always higher during crystallization under shear than after the cessation of shear. These results confirm the enhancement of growth rate due to shear-rate and the partial reduction of the growth rate after shearing. Two main facts must be noticed: a significant memory effect of the previous shear, and shear-rate, on the growth rate over a long time, and a long-time constant for the decrease of growth rate from the value observed under shear.

Overall crystallization kinetics

The overall crystallization kinetics is deduced from light intensity measurements. The transformed volume fraction α at time t, which is the volume overlapped by semi-crystalline entities (spherulites), is calculated as the ratio of the transmitted intensity to the maximum intensity obtained at the end of crystallization.

The overall crystallization kinetics at 138.5 °C and for various shear-rates are shown in Figs. 9 and 10. It clearly appears that crystallization occurs sooner and more rapidly with increasing shear-rate. This can be quantified by defining two characteristic times. First is introduced the induction time which is the time t_i corresponding to a degree of transformation $\alpha = 0.005$. Then is defined the half-transformation time which corresponds to $\alpha = 0.5$. As an effect of the very low conversion, induction time is mainly affected by nucleation event. The half-transformation time is mainly affected by a modification of growth rate. The plot of the induction time versus shear-rate is shown in Fig. 11. Induction times under shear conditions are several orders of magnitude lower than those required under quiescent conditions. Figure 11 also reveals that there is a critical shear-rate, about 10 s^{-1}, above which shear flow accelerates the crystallization process in a more efficient way. A critical shear-rate was previously reported by Lagasse and Maxwell on polyethylenes [8].

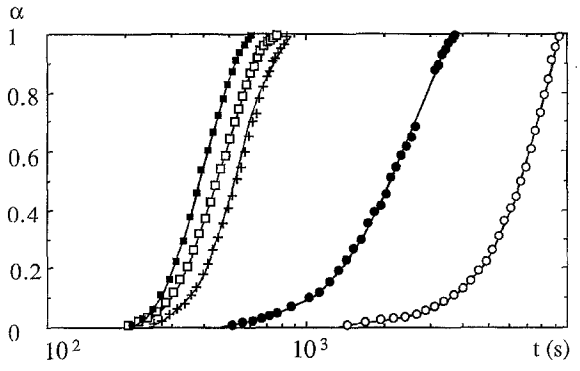

Fig. 9 Overall kinetics versus logarithm of time for various previous shear-rates, $T_c = 138.5$ °C: ○ Static, ● $\dot{\gamma} = 0.5$ s^{-1}; + $\dot{\gamma} = 1$ s^{-1}; □ $\dot{\gamma} = 1.5$ s^{-1}; ■ $\dot{\gamma} = 2$ s^{-1}

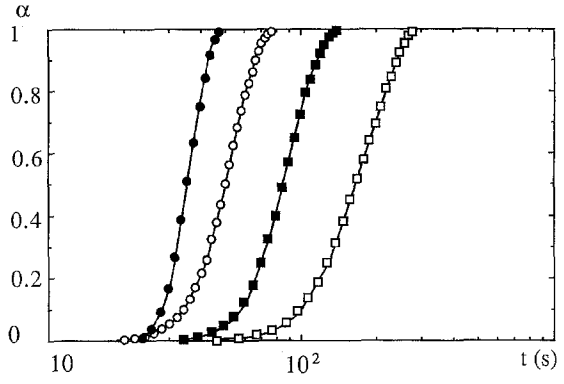

Fig. 10 Overall kinetics versus logarithm of time for various previous shear-rates, $T_c = 138.5$ °C: □ $\dot{\gamma} = 10$ s^{-1}; ■ $\dot{\gamma} = 14.6$ s^{-1}; ○ $\dot{\gamma} = 18.7$ s^{-1}; ● $\dot{\gamma} = 26$ s^{-1}

Overall crystallization kinetics have been reported above for various shear-rates at constant temperature and at constant shearing time. It is now interesting to evaluate the influence of the shearing time t_s upon the kinetics. Overall kinetics obtained at constant shear-rate and temperature are plotted in Fig. 12 for different shearing times t_s. It is concluded that the end of the kinetics is more accelerated with increasing the shearing time. But if we consider the beginning of the crystallization the induction times are not so different. The evolution of t_i versus t_s for two crystallization temperatures is plotted in Fig. 13. The induction time first decreases with increasing the shearing time and then reaches a constant value when $t_s \geq 30$ s.

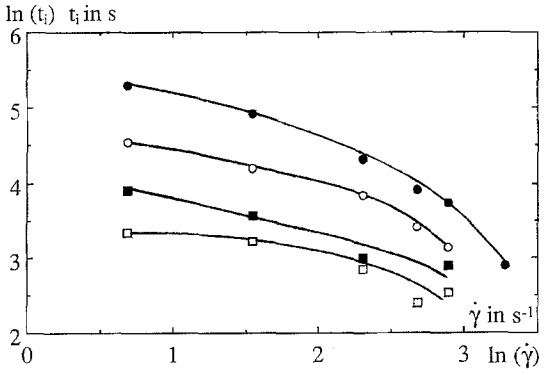

Fig. 11 Induction time versus shear-rate in a logarithm plot: □ $T_c = 130.4\,°C$; ■ $T_c = 133.9\,°C$; ○ $T_c = 136.4\,°C$; ● $T_c = 138.5\,°C$

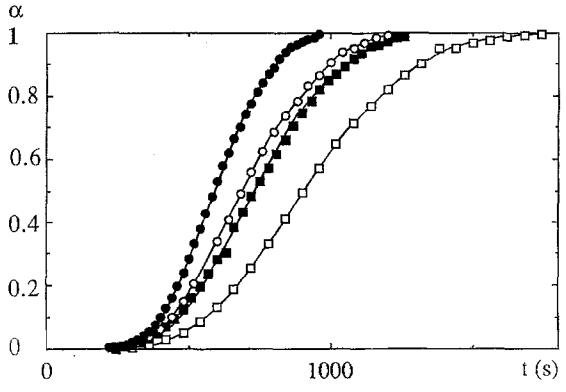

Fig. 12 Overall kinetics versus time for $\dot{\gamma} = 1\,s^{-1}$ and various previous times of shear, $T_c = 138.5\,°C$: □ $t_s = 15$ s; ■ $t_s = 30$ s; ○ $t_s = 60$ s; ● $t_s = 90$ s

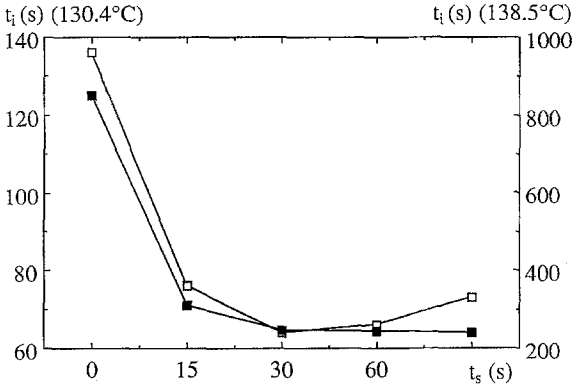

Fig. 13 Induction time t_i as a function of duration of pre-shearing t_s for $\dot{\gamma} = 1\,s^{-1}$ and two crystallization temperatures: □ $T_c = 130.4\,°C$; ■ $T_c = 138.5\,°C$

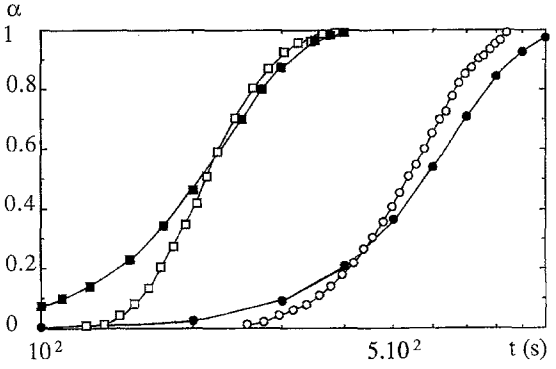

Fig. 14 Comparison of expected and effective conversions α for $\dot{\gamma} = 1\,s^{-1}$ and two crystallization temperatures: $T_c = 133.9\,°C$ (□ effective, ■ expected); $T_c = 138.5\,°C$ (○ effective, ● expected)

Data analysis and discussion

Individual measurements of nucleation and growth rates as well as measurements of the overall kinetics exhibit a significant enhancement of all the kinetics due to a previous shear-rate. Correlation between elementary mechanisms (nucleation and growth) and overall kinetics will be first considered in order to demonstrate the consistency of our results. For that purpose, Avrami–Evans' equation [22–25] will be used to describe the overall kinetics. In the general form of this equation, the volume fraction $\alpha(t)$ transformed at time t is written as:

$$\alpha(t) = 1 - \exp[-E(t)] \,. \tag{3}$$

A very simple form of $E(t)$ is predicted for spherulites growing from instantaneously activated nuclei, if we assume that the density of potential nuclei can be approximated by the final density of activated nuclei N_{af}:

$$E(t) = \frac{4}{3}\pi N_{af} G^3 t^3 \,. \tag{4}$$

The growth rate G and the density of activated nuclei N_{af} are directly measured in our experiments (see the section "Results") and used to calculate the transformed fraction (or conversion) $\alpha(t)$. This expected conversion is compared with effective values in Fig. 14 from data reported in Table 3. A rather good agreement is obtained for the two different crystallization temperatures in spité of the poor precision of the calculation due to the experimental uncertainty on N_{af} and G values. The important hypothesis of initial (or instantaneous) nucleation will be justified during the discussion on nucleation event. Nevertheless, it can already be noticed from the comparison of Figs. 4 and 9 that most of the nuclei are activated at the very beginning of the transformation, which is consistent with the assumption of an initial nucleation. The best agreement is observed from a conversion α greater than 0.2. The reasons of this better agreement will also be discussed later. Consequently, using a number of assumptions, it is possible to relate the overall kinetics to

Table 3 Effect of a previous shear-rate on the growth rate and the nucleation density

Crystallization temperature	$\dot{\gamma}$ s^{-1}	G μm s^{-1}	N_{af} nuclei mm^{-3}
133.9 °C	0	0.080	180
	1	0.100	18 500
138.5 °C	0	0.026	80
	1	0.038	15 700

parameters describing the elementary processes of nucleation and growth.

The enhancement of the nucleation process produced by shear flow has been previously reported. Fritzsche et al. have noticed an increase of the nucleation rate of polyethylene oxide [9]. Wolkowicz has reported the same effect for polybutene-1 [12]. The present results are analyzed with the kinetic models for heterogeneous nucleation proposed by Binsbergen [26]. According to the nucleation mode, the nucleation rate can be written as:

$$\frac{dN_a}{dt} = \dot{N}_0 \exp\left(-\frac{\Delta G_t}{kT_c}\right)\exp\left(-\frac{K_i}{T_c \Delta T}\right) \tag{5}$$

or

$$\frac{dN_a}{dt} = \dot{N}_0 \exp\left(-\frac{\Delta G_t}{kT_c}\right)\exp\left(-\frac{K_i'}{T_c \Delta T^2}\right), \tag{6}$$

where $\dot{N}_0$ is a pre-exponential factor, ΔG_t is the activation energy for interfacial transport, K_i and K_i' are the nucleation parameters, k is the Boltzmann constant. ΔT is the undercooling related to the equilibrium melting temperature T_m^0 ($\Delta T = T_m^0 - T_c$). For crystallization of polymers from the melt, ΔG_t is usually given by the Suzuki–Kovacs equation [27]

$$\frac{\Delta G_t}{kT_c} = \frac{U^*}{R(T - T_\infty)}, \tag{7}$$

where R is the gas constant, $U^* = 6270$ J/mol and $T_\infty = T_g - 30$ °C, $T_g = -21$ °C being the glass transition temperature. Equation (6) can describe homogeneous nucleation with a special form for the nucleation parameter, $K_i' = K_I$:

$$K_I = \frac{32\sigma^2\sigma_e T_m^{02}}{k\Delta h^2}, \tag{8}$$

where σ and σ_e are the surface energies of the lateral and fold surfaces, respectively, and Δh is the heat of fusion per unit volume. The numerical values used in the calculations are the following: $\sigma = 8\ 10^{-7}$ J/cm^2, $\sigma_e = 1.4\ 10^{-5}$ J/cm^2, $\Delta h = 140$ J/cm^3, $T_m^0 = 481$ K. The values of these thermodynamical parameters are deduced from a previous study of a homopolymer [17, 21] and applied here since the present copolymer seemingly behaves as a homopolymer concerning the crystallization phenomena. In a classical way, the equilibrium melting temperature T_m^0 is defined as the temperature at which the curve giving the melting temperature T_m versus the crystallization temperature T_c intersects the straight line $T_m = T_c$. Δh is obtained by extrapolation to T_m^0 of the curve giving the enthalpy of fusion per unit unit mass versus T_c, and then conversion into enthalpy of fusion per unit volume, σ is given by a semi-empirical expression, and finally, σ_e is deduced from the interpretation of growth-rate data (Eqs. (9) and (10) below). Our calculations clearly show that the nucleation of this copolymer is heterogeneous for quiescent condition. It is difficult to precisely determine the type of substrate (coherent or non-coherent) activated and the thermodependence of the nucleation rate, the thermal dependence being too low compared with the uncertainty on the measurements (see "Results" and Fig. 6). Thus, we are inclined to favor Eq. (5) because in such a case the variations of the nucleation rate and the growth rate with temperature under static condition are identical ($K_i = K_g = 6.5\ 10^5$ K^2), where K_g is defined below by Eqs. (9) and (10). This is consistent with analogous mechanisms for the deposit of molecular segments on the crystalline substrate. However, Eq. (6) would also lead to acceptable results.

The nucleation parameter K_i can be deduced from the induction time t_i measured during experiments performed under the same shear-rate at different temperatures (Eq. (5), Figs. 15 and 16). This treatment assumes that the induction time is proportional to the reciprocal of the nucleation rate and that the equilibrium melting temperature is not modified by shear-rate. At any temperature the value of the K_i parameter is the same in static condition and at $\dot{\gamma} = 0.5$ s^{-1}. Therefore, the nucleation seems to be unmodified from static condition up to this critical shear-rate. This critical shear-rate for nucleation event is the same as the one directly observed by optical microscopy (see "Results" and Fig. 6). Above $\dot{\gamma} = 0.5$ s^{-1} the apparent K_i decreases when the shear-rate increases. The decrease of the activation parameter K_i is consistent with the increase of the density of activated nuclei and of the nucleation rate (Figs. 4 and 6). This activation parameter is related to the free energy difference between the potential nuclei and the polymer melt, here oriented by the shear. Heterogeneous nucleation observed under static condition seems to remain heterogeneous under shear flow. Two experimental facts observed on polypropylene argue for this conclusion: homogeneous nucleation was observed in quiescent condition only below $T_c = 85$ °C [28, 29], almost 45 °C lower than in the present work, and the K_i value predicted by homogeneous nucleation theory is much more higher than

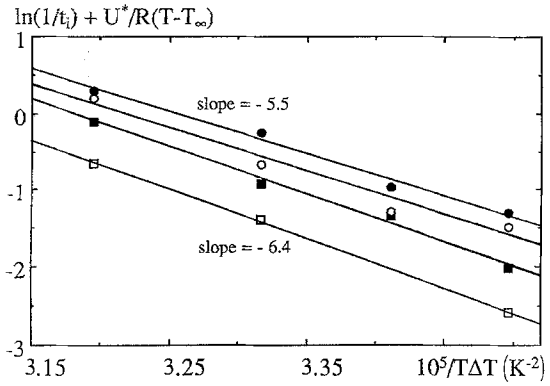

Fig. 15 Comparison of nucleation parameter K_i deduced from static experiments and after previous shear-rates performed under various isothermal conditions: □ Static; ■ $\dot{\gamma} = 0.5\ s^{-1}$; ○ $\dot{\gamma} = 1\ s^{-1}$; ● $\dot{\gamma} = 2\ s^{-1}$; induction time in s

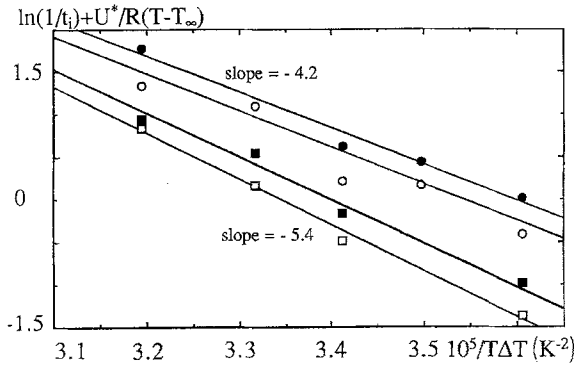

Fig. 16 Measurement of nucleation parameter K_i after previous shear-rates performed under various isothermal conditions: □ $\dot{\gamma} = 2\ s^{-1}$; ■ $\dot{\gamma} = 4.7\ s^{-1}$; ○ $\dot{\gamma} = 10\ s^{-1}$; ● $\dot{\gamma} = 14.6\ s^{-1}$; induction time in s

the present data [28, 29]. Consequently, we conclude that the nucleation under shear is still heterogeneous but with a lowering of the activation parameter K_i when the shear-rate increases.

The growth rates measured under static condition and after shear are analyzed with the kinetic model proposed by Lauritzen and Hoffman [30]. Although it is generally admitted that crystalline growth in polymers is governed by a nucleation mechanism (see for instance [31]), many serious objections have been raised to the Lauritzen–Hoffman theory in the literature (see for instance [32]). The discussion of these objections is beyond the scope of the present paper, and the Lauritzen–Hoffman equation will be simply used as a convenient way to fit the experimental data. In this equation, the growth rate G is written as:

$$G = G_0 \exp\left(-\frac{\Delta G_t}{kT_c}\right)\exp\left(-\frac{K_g}{T_c \Delta T}\right), \qquad (9)$$

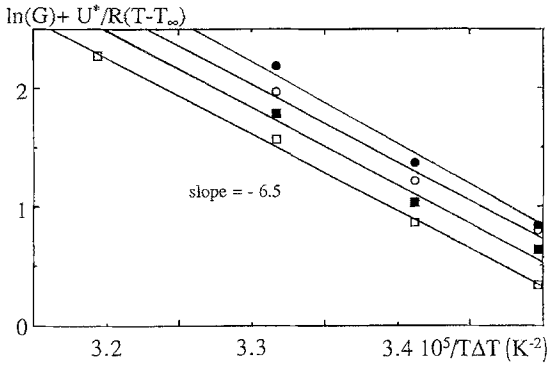

Fig. 17 Comparison of growth-rate parameter K_g deduced from static experiments and after previous shear-rates performed under various isothermal conditions: □ Static; ■ $\dot{\gamma} = 1\ s^{-1}$; ○ $\dot{\gamma} = 1.5\ s^{-1}$; ● $\dot{\gamma} = 2\ s^{-1}$; growth rate in $\mu m\ s^{-1}$

where K_g is defined as:

$$K_g = \frac{Y b_0 \sigma \sigma_e T_m^0}{k \Delta h} \qquad (10)$$

with $Y = 4$ for regimes I and III and $Y = 2$ for regime II [33]; b_0 is the monolayer thickness (here $b_0 = 0.6$ nm). The growth rate data are analyzed with Eqs. (7) and (9) (Fig. 17). The K_g parameter, i.e., the opposite of the slope of the straight line in the $\ln(G) + \Delta G_t/kT_c$ versus $1/T_c\Delta T$ plot, obtained under shear condition, is the same as for the quiescent one. It has almost the same value as the one measured under static condition in the same temperature range on polypropylene homopolymer [17, 21]. These results confirm once more that this polymer behaves as a homopolymer and then imply that shear does not change either the surface energies σ and σ_e, or the Y parameter ($Y = 4$ in this temperature range [17, 21]). Only the ordinate G_0 is modified by shear if we assume no change of the equilibrium melting temperature T_m^0 (Fig. 17). The same results can be analyzed with only a change of T_m^0 without any change of G_0, but this second type of treatment requires the use of a theoretical model to calculate the variation of T_m^0 with applied shear-rate. Such a treatment, which can be found in ref. [14], is beyond the scope of the present paper, and, consequently, as for the treatment of nucleation event, only "apparent" values of K_i and K_g will be considered.

This thermal dependence of growth rate can also be analyzed with overall experiments under higher shear-rates (Fig. 18). If the induction time mainly results from nucleation event, the time for half-transformation $t_{0.5}$ is highly dependent on growth rate. We assume that this time $t_{0.5}$ is inversely proportional to the growth rate. Then, the K_g parameter should be deduced from the plot of $1/t_{0.5}$

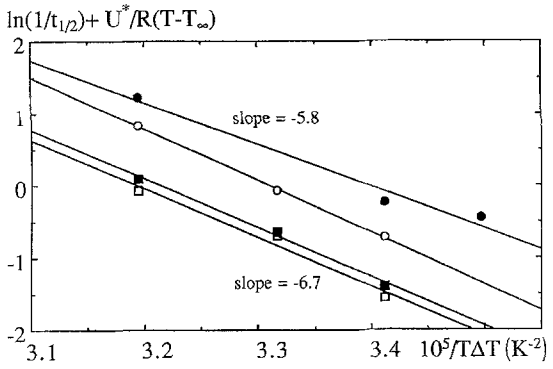

Fig. 18 Measurement of growth-rate parameter K_g deduced from the time for half-transformation: □ $\dot{\gamma} = 2\ s^{-1}$; ■ $\dot{\gamma} = 5\ s^{-1}$; ○ $\dot{\gamma} = 10\ s^{-1}$; ● $\dot{\gamma} = 14.6\ s^{-1}$; time for half-conversion in s

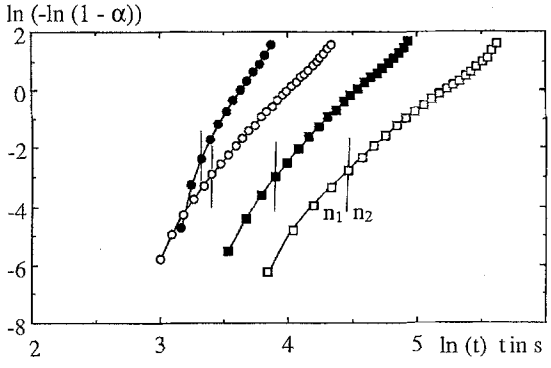

Fig. 19 Measurement of Avrami exponent according to Eq. (11) for $T_c = 138.5\,°C$ and after various shear-rates: □ $\dot{\gamma} = 10\ s^{-1}$; ■ $\dot{\gamma} = 14.6\ s^{-1}$; ○ $\dot{\gamma} = 18.7\ s^{-1}$; ● $\dot{\gamma} = 26\ s^{-1}$

versus $1/T_c\Delta T$ (Fig. 18). Straight lines, significant of the different shear-rates, are observed up to the highest available shear-rate $\dot{\gamma} = 15\ s^{-1}$. The slope of these lines ($-K_g$) varies but remains close to the value determined in the low shear-rate range and under static condition. Therefore, it can be inferred that the mechanisms controlling growth rate are not modified by a previous shear-rate.

Nucleation and growth kinetics exhibit an effect of a previous shearing. The effect of this previous shear will be specifically considered on the parameters of the overall kinetics (with a simplified form of the Avrami–Evans equation):

$$\alpha = 1 - \exp[-kt^n], \tag{11}$$

where n is the Avrami exponent and k is a kinetic parameter function of the isothermal crystallization temperature. Both parameters are related to the elementary mechanisms of nucleation and growth. The Avrami exponent n is deduced from the slope of the double logarithm plot $\ln[-\ln(1-\alpha)]$ vs. $\ln(t)$, as represented in Fig. 19. For a spherulitic growth controlled by an interfacial process the n exponent must be in the range $3 \leq n \leq 4$, when the nucleation changes from initial to sporadic in time, respectively.

As is usual, for each static crystallization of this polymer, the whole kinetics can be described by only one Avrami exponent with the value $n = 3 \pm 0.1$, which is characteristic of an initial nucleation. Consequently, the heterogeneous nucleation is initial in static condition. Surprisingly, two successive exponents are necessary to represent the kinetics measured after shear. During the first step of the transformation ($\alpha < 0.2$), the values of the Avrami exponent are too high ($n > 4$) with respect to the values predicted by the usual models, while the values of the second exponent are very similar to those deduced from static conditions, excepted for some cases at high shear-rates. It is the main reason why only data deduced from the second stage were considered for the comparison with nucleation and growth kinetics. The too high value of the first Avrami exponent remains unusual. It appears to be temperature sensitive and increasing with shear-rate (Table 4). A so high exponent was previously observed during crystallization under shear. Sherwood et al. [13] have already reported an exponent n greater than 5 for crystallization of polyethylene oxide under shear. Fritzsche and Price [6] suggested that the shear stress could disrupt the crystalline aggregates, which leads to a "pseudo-homogeneous nucleation". The sudden injection of nuclei could yield an apparent increase of the Avrami exponent as we observe, but we conclude that the nucleation remains heterogeneous. In our experiments homogeneous nucleation is highly non-probable, as discussed above. The sudden increase of nuclei appears in the first step of the crystallization (compare time scales for nucleation (Fig. 4) and for the over all kinetics (Fig. 9)).

Table 4 The two successive Avrami exponents measured after shear as a function of temperature and shear-rate

Crystallization temperature	$\dot{\gamma}\ s^{-1}$	n_1	n_2
130.4 °C	0.5	5.5	3.6
	1	6.1	2.7
	2	7.3	4.2
	4.7	8.2	4.7
	10.0	12.1	8.1
	14.6	11.0	7.1
	18.7	10.9	7.1
138.5 °C	0.5	4.1	3.5
	1	5.3	3.4
	2	5.7	4
	10.0	4.5	3.4
	14.6	5.2	3.9

Colloid & Polymer Science, Vol. 274, No. 3 (1996)

During the second part, in which the Avrami coefficient n_2 is measured, the nucleation density remains almost constant. These conditions are consistent with the hypothesis of an initial nucleation for this crystallization period, as previously assumed for the prediction of the overall kinetics. It must be noticed that very dispersed values of n are deduced from kinetic experiments under shear. Tan and Gogos [7] have found that the Avrami exponent could vary from 3 to 1 for the same experiment. In contrast with our results where the spherulitic morphology is always observed, this fact is predicted by Avrami's formalism when the morphologies reduce their symmetry of growth from sphere to unidimensional entity. This analysis is consistent with morphological observations of transverse growth from row nuclei [3]. This effect of row nucleation on growth anisotropy of polyethylene under shear was more recently discussed, as well as its effect on the Avrami exponent [19]. In our experiments on polypropylene no growth anisotropy was observed from essentially random nucleation in the volume, the morphology being spherulitic. The strong increase of random nuclei at the beginning of the experiment is the main feature which seems to induce the strong increase of n_1 over 4 in the first step of crystallization.

Conclusion

The analysis of the crystallization of this polypropylene under and after shear shows that the main mechanisms of nucleation and growth are not basically modified with respect to static condition, for the range of shear-rates investigated here. The nuclei seem to be randomly distributed in the sample and induce a spherulitic growth. The nucleation remains heterogeneous and the crystalline growth mechanism remains interfacial during the experiments. The two main differences with the static condition are a very strong increase of the nucleation density and an enhancement of the growth rate. The strong increase of the nucleation density in the first part of the crystallization event mainly explains a very high value of the Avrami exponent, well above $n = 4$. Then, the second step of the overall kinetics can be described by a more usual form of Avrami's theory. Even when the crystallization occurs after shear, the growth rate is larger than in a quiescent condition. This fact results from an only partial relaxation of the orientation induced by shear. This is not obviously expected because shear is not generally recognized to induce a sufficient orientation and because the relaxation is very long, i.e., several tenths of seconds. The beginning of a partial relaxation of growth rate is observed during the first seconds after cessation of shear. The second step of the overall kinetics can be calculated from the nucleation density and from the growth rate measured in the same period of time.

At high shear-rate and/or at low temperature, the perturbations due to flow become more and more important, and one tends to pass from a crystallization after shear to a crystallization under shear. This assessment is attested by several experimental facts: the decrease of the induction time is sharper above $\dot{\gamma} = 10\ s^{-1}$ (Fig. 11), high values of the Avrami exponent n_2 are obtained at 130.4 °C when shear-rate increases (Table 4), and finally shear experiments cannot be achieved below 130 °C because of the rapid crystallization under shear.

References

1. Pennings AJ, Van der Mark JMAA, Booij HC (1970) Kolloid ZZ Polym 236:99
2. Haas TW, Maxwell B (1969) Polym Eng Sci 9:225
3. Kobayashi K, Nagasawa J (1970) J Macromol Sci Phys B 4(2):331
4. Wereta A, Gogos C (1971) Polym Eng Sci 11:19
5. Krueger D, Yeh GSY (1972) J Appl Phys 43:4339
6. Fritzsche AK, Price FP (1974) Polym Eng Sci 14:401
7. Tan V, Gogos C (1971) Polym Eng Sci 11:512
8. Lagasse RR, Maxwell B (1976) Polym Eng Sci 16:189
9. Fritzsche AK, Price FP, Ulrich RD (1976) Polym Eng Sci 16:182
10. Ulrich RD, Price FP (1976) J Appl Polym Sci 20:1077
11. Andersen PG, Carr SH (1978) Polym Eng Sci 18:215
12. Wolkowicz MD (1978) J Polym Sci, Polym Symp 63:365
13. Sherwood CH, Price FP, Stein RS (1978) J Polym Sci, Polym Symp 63:77
14. Tribout C (1993) Thesis, Ecole Nationale Supérieure des Mines de Paris
15. Mirabella FM Jr (1993) Polymer 34: 1729
16. Monasse B (1982) Thesis, Ecole Nationale Supérieure des Mines de Paris
17. Monasse B, Haudin JM (1985) Colloid Polym Sci 263:822
18. Monasse B, Fryda C (1990) 6th Annual Meeting of the Polymer Processing Society, Nice
19. Monasse B (1995) J Mater Sci 30:5002
20. Monasse B (1992) J Mater Sci 27:6047
21. Monasse B (1987) Thesis, Université Claude Bernard (Lyon I)
22. Avrami M (1939) J Chem Phys 7:1103
23. Avrami M (1940) J Chem Phys 8:212
24. Avrami M (1941) J Chem Phys 9:177
25. Evans UR (1945) Trans Faraday Soc 41:365
26. Binsbergen FL (1973) J Polym Sci, Polym Phys Ed 11:117
27. Suzuki T, Kovacs AJ (1970) Polym J 1:82
28. Koutsky JA, Walton AG, Baer E (1967) J Appl Phys 38:1832
29. Burns JR, Turnbull D (1966) J Appl Phys 37:402
30. Lauritzen JI Jr, Hoffman JD (1960) J Res Natl Bur Stand 64A:73
31. Mandelkern L (1993) The Crystalline State in "Physical Properties of Polymers", 2nd edition, American Chemical Society, Washington DC
32. Point JJ, Colet MC (1990) Ann Chim Fr 15:221
33. Hoffman JD (1983) Polymer 24:3